Second Coordination Shell Water Exchange Rate and Mechanism: Experiments and Modeling on Hexaaquachromium(III)

A. Bleuzen,[†] F. Foglia,[†] E. Furet,[‡] L. Helm,*[,†] A. E. Merbach,*[,†] and J. Weber[‡]

Contribution from the Institut de Chimie Minérale et Analytique, Université de Lausanne, Bâtiment de Chimie (BCH), CH-1015 Lausanne, Switzerland, and Département de Chimie Physique, Université de Genève, 30 quai Ernest-Ansermet, CH-1211 Genève 4, Switzerland

Received April 22, 1996[⊗]

Abstract: From our combined experimental and computer modeling study we found a structurally and kinetically well-defined second coordination shell around chromium(III) ions in aqueous solution. Strong hydrogen binding due to polarization of first coordination sphere water molecules leads to a mean coordination number of 12.94 water molecules in the second shell and to short first shell hydrogen−second shell oxygen distances of about 1.4 Å. The experimentally measured exchange rate constant of $k_{ex}^{298} = (7.8 \pm 0.2) \times 10^9$ s^{-1} ($\Delta H^{\ddagger} = 21.3 \pm 1.1$ kJ mol^{-1}, $\Delta S^{\ddagger} = +16.2 \pm 3.7$ J K^{-1} mol^{-1}) corresponds to a lifetime of 128 ps for one water molecule in the second coordination shell and compares very well with a lifetime of 144 ps as observed from molecular dynamics simulation of a $[Cr(H_2O)_6]^{3+}$ complex in aqueous solution. The geometry and the partial atomic charges of $[Cr(H_2O)_6]^{3+}$ were determined by density functional theory (DFT) calculations. Water exchange from the second coordination shell to the bulk of the solution proceeds between a H_2O sitting in the second shell and an adjacent one which just entered this shell from the bulk. By a small rotation of the first coordination shell water molecule, one of its two hydrogen bonds jumps to the entered water molecule and the one which lost its hydrogen bond leaves the second shell of the $[Cr(H_2O)_6]^{3+}$. This associative reaction mode is a model for water exchange between water molecules which are bound by strong hydrogen bonds, as in the case for strongly polarizing 3+ ions such as Al^{3+} or Rh^{3+}. Furthermore, the exchange phenomenon between second sphere and bulk water involving only two adjacent water molecules is strongly localized and independent of other water molecules of the second shell. In this respect it may be considered as a starting point for a study of water exchange on a protonated metal oxide surface.

Introduction

It is a common approach in chemistry to separate solvent molecules around a metal ion in solution into different coordination or solvation shells.[1] The first coordination shell (or coordination sphere) consists of solvent molecules which are immediate neighbors of the ion. The second coordination shell includes all solvent molecules forming neighbors to those in the first shell and having some properties which makes them distinguishable from pure solvent molecules. Solvent molecules having no such distinguishable properties, and in general all of them outside the second coordination shell, are regarded as *bulk solvent*. Solvent molecules in the first coordination sphere interact, depending on the nature of the metal ion and the solvent itself, more or less strongly with the ionic center. This is clearly demonstrated by the enormous variation in lifetime of water molecules in the first coordination sphere of 3+ ions: Experimentally found lifetimes extend over 19 orders of magnitude from 9.1×10^9 s for $[Ir(H_2O)_6]^{3+}$ [2] to 1.2×10^{-9} s for $[Gd(H_2O)_8]^{3+}$.[3] The number of water molecules (coordination number, CN) in the first shell varies from 4 (Li^+, Be^{2+}) to 9 (Nd^{3+}). Due to developments in experimental techniques such as high-field and high-pressure NMR,[4] neutron diffraction (first-order difference technique[5]) or EXAFS (extended X-ray absorption fine structure),[6] the knowledge about the structure and the dynamics of the first coordination shell has increased dramatically in the last two decades.[7]

The knowledge on the second coordination sphere is scarce. Properties of solvent molecules in this coordination shell are often very similar to those of the bulk, making their investigation extremely difficult. Ions having a kinetically inert first coordination shell offer the best opportunity. Among them the strongly paramagnetic aqua ion of chromium(III) is the most suitable. Structural data of $[Cr(H_2O)_6]^{3+}$ in the solid state and in solution are summarized in Table 1.[8−19] From diffraction

* To whom correspondence should be addressed.
† Université de Lausanne.
‡ Université de Genève.
⊗ Abstract published in *Advance ACS Abstracts,* December 1, 1996.

(1) Marcus, Y. *Ion solvation*; John Wiley & Sons: Chichester, 1985.
(2) Cusanelli, A.; Frey, U.; Richens, D. T.; Merbach, A. E. *J. Am. Chem. Soc.* **1996**, *118*, 9333.
(3) Micskei, K.; Powell, D. H.; Helm, L.; Brücher, E.; Merbach, A. E. *Magn. Reson. Chem.* **1993**, *31*, 1011.
(4) Frey, U.; Merbach, A. E.; Powell, D. H. *Solvent Exchange on Metal Ions: A Variable Pressure NMR Approach* In: *Dynamics of Solutions and Fluid Mixtures by NMR*; John Wiley & Sons: Chichester, 1995.
(5) Enderby, J. E. *Chem. Soc. Rev.* **1995**, *24*, 159
(6) Koningsberger, D. C., Prins, R., Eds. *X-Ray Absorption: Principles, Applications, Techniques of EXAFS, SEXAFS and XANES*; Wiley: New York, 1988.
(7) (a) Ohtaki, H.; Radnai, *T. Chem. Rev.* **1993**, *93*, 1157. (b) Lincoln, S. F.; Merbach, A. E. Substitution Reactions of Solvated Metal Ions. *Advances in Inorganic Chemistry*; Academic Press: New York, 1995; Vol. 42, p 1.
(8) Read, M. C.; Sandström, M. *Acta Chem. Scand.* **1992**, *46*, 1177.
(9) Caminiti, R.; Licheri, G.; Piccagula, G.; Pinna, G. *J. Chem. Phys.* **1978**, *69*, 1.
(10) Bol, W.; Welzen, T. *Chem. Phys. Lett.* **1977**, *49*, 189.
(11) Magini, M. *J. Chem. Phys.* **1980**, *73*, 2499.
(12) Broadbent, R. D.; Neilson, G. W.; Sandström, M. *J. Phys.: Condens. Matter* **1992**, *4*, 639.
(13) Munoz-Páez, A.; Pappalardo, R. R.; Sanchez-Marcos, E. *J. Am. Chem. Soc.* **1995**, *117*, 11710−11720.
(14) Schein, B. J. B.; Lingafelter, E. C.; Stewart, J. M. *J. Phys. Chem.* **1967**, *47*, 5183.

S0002-7863(96)01311-X CCC: $12.00

Table 1. Experimental and Calculated Structural Data for $[Cr(H_2O)_6]^{3+}$

	concn	Cr−O_I[a]/Å	Cr−O_{II}[b]/Å	Cr−H_{II}[c]/Å	CN_{II}[d]	method[e]	ref
aqueous $Cr(ClO_4)_3/Rh(ClO_4)_3$	1 M	2.03 ± 0.02	4.02 ± 0.02		13 ± 1	LAXS	8
aqueous $CrCl_3$	1 M	1.994(3)	4.05(2)		12	XRD	9
aqueous $Cr(NO_3)_3$	1 M	1.999(3)	4.08(1)		12	XRD	
aqueous $Cr(NO_3)_3$	2 M	1.989(3)	4.06(2)		12	XRD	
aqueous $Cr(NO_3)_3$	0.5 M	1.98	4.20−4.25			XRD	10
aqueous $CrCl_3$	0.66 M	1.97(1)				XRD	11
aqueous $Cr(ClO_4)_3$	2.2 M	1.98(2)	4	4.5	12.0(4)	ND	12
aqueous $Cr(NO_3)_3$	2.6 *m*	2.01 ± 0.008	3.95 ± 0.06		13.1 ± 0.9	EXAFS	13
	1.5 *m*	2.01 ± 0.008	3.95 ± 0.05		13.1 ± 0.8	EXAFS	
	0.1 *m*	2.00 ± 0.01	3.96 ± 0.08		13.6 ± 1.4	EXAFS	
	0.05 *m*	2.00 ± 0.01	3.97 ± 0.08		13.4 ± 1.3	EXAFS	
	0.01 *m*	2.01 ± 0.01	4.02 ± 0.08		13.5 ± 1.2	EXAFS	
	0.005 *m*	2.01 ± 0.01	4.00 ± 0.08		13.6 ± 1.0	EXAFS	
$C(NH_2)_3[Cr(H_2O)_6](SO_4)_2$		1.950				XRD	14
$(NH_4)_2[Cr(H_2O)_6]F_5$		1.966				XRD	15
$Cs[Cr(H_2O)_6](SO_4)_2 \cdot 6H_2O$		1.959(3)				XRD	16
$NH_2(CH_3)_2[Cr(H_2O)_6](SO_4)_2$		1.960				XRD	17
$Cs[Cr(H_2O)_6](SO_4)_2 \cdot 6H_2O$		1.961(2)				ND	18
calculation, $[Cr(H_2O)_6]^{3+}$		2.025				SCF	8
calculation, $[Cr(H_2O)_6]^{3+} \cdot H_2O$		2.050	4.06	4.49	14	SCRF/MC	19
calculation, $[Cr(H_2O)_6]^{3+}$		1.956				DFT/LDA	this work
calculation, $[Cr(H_2O)_6]^{3+}$		2.005				DFT/NLDA	this work

[a] Distance between the chromium ion and the oxygen atoms O_I of the first shell. [b] Distance between the chromium ion and the oxygen atoms O_{II} of the second shell. [c] Distance between the chromium ion and the hydrogen atoms H_{II} of the second shell. [d] Second shell coordination number. [e] LAXS = large angle X-ray diffraction; XRD = X-ray diffraction; ND = neutron diffraction; EXAFS = X-ray extended X-ray absorption fine structure; SCF = self-consistent field; SCRF = self-consistent reaction field; MC = Monte Carlo simulation; DFT = density functional theory.

experiments and from a recent Monte Carlo simulation[19] of Cr^{3+} in water using an ab initio intermolecular potential, it can be concluded that the chromium(III) in aqueous solution has a well-structured second coordination sphere composed of 12−14 water molecules. Further evidence for a rather strong second solvation shell of Cr^{3+} was found from infrared spectroscopy[20] which showed formation of strong hydrogen bonds between the first and second coordination shells.

Information on the kinetic behavior of second sphere water molecules is even more scarce. Easteal et al.[21] used a three-site model ($[Cr(H_2O)_6]^{3+}$, second shell water, bulk water) to describe their tracer diffusion coefficient measurements. Diffusion coefficients of second shell water molecules were found to lay between that of the first shell and bulk water. An incoherent quasi-elastic neutron scattering study on aqueous Cr^{3+} perchlorate solutions[22] resulted in a Cr^{3+} second shell water−proton binding time of $<5 \times 10^{-9}$ s. A molecular dynamics simulation study on aqueous lanthanide(III) ions[23] gave residence times of water molecules in the second coordination sphere of $(12-18) \times 10^{-12}$ s. Olson[24] and Earl[25] in early attempts tried to measure H_2O lifetimes in the second sphere of Cr^{3+} using ^{17}O NMR. Their residence times, on the order of 100 ps, are about 1 order of magnitude larger than the simulation result on Ln^{3+} ions.

Experimental Section

Materials and Sample Preparation. Rhodium(III) chloride hydrate (Fluka, puriss), 70% perchloric acid (Merck, pa), and ^{17}O-enriched water (2 atom %, Yeda) were used as received. Chromium(III) perchlorate (Alfa products) was partially redried before use. The chromium content of the solutions was checked by atomic absorption. $[Rh(H_2O)_6](ClO_4)_3$ complex was prepared by reaction of aqueous $RhCl_3$ with 70% perchloric acid according to the procedure of Ayres and Forrester.[26] $[Cr(H_2O)_6](ClO_4)_3$ and $[Rh(H_2O)_6](ClO_4)_3$ stock solutions were prepared by dissolving the salts in acidic ^{17}O-enriched water. The molalities of the solutions are, respectively, 0.84 in $[Cr(H_2O)_6]^{3+}$ and 0.83 in $[Rh(H_2O)_6]^{3+}$, and 0.2 in $HClO_4$ in both cases. The rhodium solution was heated at 80 °C for two days in ^{17}O-enriched water to complete the enrichment.[27]

The samples were prepared by mixing different weighted amounts of the stock solutions, leading to solutions with constant acidity (0.2 M in $HClO_4$) and ionic strength ($\mu \cong 1$). The molalities (mol of $Cr(H_2O)_6$/kg of solvent) of the five samples used are 0.203, 0.277, 0.415, 0.559, and 0.84 of $[Cr(H_2O)_6](ClO_4)_3$, respectively. If the number of water molecules in the second coordination sphere of Cr^{3+} is assumed to be 12, mole fractions of second sphere water molecules can be calculated to be 0.044, 0.060, 0.090, 0.121, and 0.182 for the five samples, respectively.

Instrumentation and NMR Measurements. Variable-temperature ^{17}O NMR measurements were performed at two magnetic fields with Bruker AMX-600 (14.1 T, 81.3 MHz) and Bruker AM-400 (9.4 T, 54.2 MHz) spectrometers using 10 mm od sample tubes. Bruker VT-2000 temperature control units were used to stabilize the temperature, which was measured by a substitution technique.[28]

Longitudinal relaxation rates, $1/T_1$, were obtained by the

(15) Massa, W. *ZAACA* **1977**, *436*, 29.
(16) Beattie, J. K.; Best, S. P.; Skelton, B. W.; White, A. H. *J. Chem. Soc., Dalton Trans.* **1981**, 2105.
(17) Galesic N.; Jordanovska, V. B. *Acta Crystallogr., C* **1992**, *48*, 256.
(18) Best, S. P.; Forsyth, J. B. *J. Chem. Soc., Dalton Trans.* **1991**, 1721.
(19) Pappalardo, R. R.; Martínez, J. M.; Marcos, E. S. *J. Phys. Chem.* **1996**, *100*, 11748.
(20) Bergström, P.; Lindgren, J.; Read, M. C.; Sandström, M. *J. Phys. Chem.* **1991**, *95*, 7650.
(21) Easteal, A. J.; Mills, R.; Woolf, L. A. *J. Phys. Chem.* **1989**, *93*, 4968.
(22) Salmon, P. S.; Herdman, G. J.; Lindgren, J.; Read, M. C.; Sandström, M. *J. Phys.: Condens. Matter* **1989**, *1*, 3459.
(23) Kowall, Th.; Foglia, F.; Helm, L.; Merbach, A. E. *Chem. Eur. J.* **1996**, *2*, 131.
(24) Olson, M. V.; Kanazawa, Y.; Taube, H. *J. Chem. Phys.* **1969**, *51*, 289.
(25) Earl, W. L. Ph.D. Thesis, University of California, 1975.
(26) Ayres, H. R.; Forrester, J. S. *J. Inorg. Chem.* **1957**, *3*, 365.
(27) Laurenczy, G.; Rapaport, I.; Zbinden, D.; Merbach, A. E. *Magn. Reson. Chem.* **1991**, *29*, S45.
(28) Amman, C.; Meyer, P.; Merbach, A. E. *J. Magn. Res.* **1982**, *46*, 319.

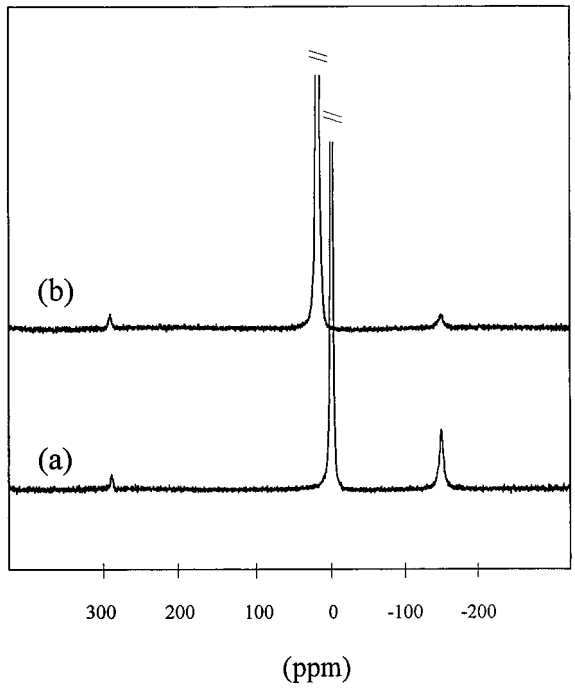

Figure 1. 81.33 MHz oxygen-17 NMR spectra of (a) an aqueous solution 0.84 *m* in $Rh(ClO)_4)_3$ and (b) an aqueous solution 0.281 *m* in $Rh(ClO)_4)_3$ and 0.559 *m* in $Cr(ClO)_4)_3$ in 2% enriched H_2O at 286 K.

inversion−recovery method[29], and transverse relaxation rates, $1/T_2$, were measured by the Carr−Purcell−Meiboom−Gill spin echo technique.[30] The sweep width used was 70 000 Hz (2500 Hz) for chemical shift (relaxation) measurements, and 2000 (24) transients of 4K (1K) data points were added prior to Fourier transformation.

The water molecules of the rhodium(III) first coordination sphere were used as an internal reference for chemical shift measurements. $[Rh(H_2O)_6]^{3+}$ was chosen because its chemical properties are very similar to those of $[Cr(H_2O)_6]^{3+}$: same electric charge, comparable size, and very long lifetime of water oxygens in the primary coordination shell. The lifetime of the water oxygen is about 10^6 s for chromium[31−33] and 5×10^8 s for rhodium[27] at room temperature. It has also recently been shown that the hexahydrated metal ions of chromium and rhodium are essentially isostructural with respect to their solvation structures in aqueous solution.[8,20] It can therefore be expected that the presence of $[Rh(H_2O)_6]^{3+}$ does not change solution properties in the vicinity of the chromium ions. Furthermore, no interaction between chromium and the internal reference such as ion pairing or complexation is expected.

Three ^{17}O NMR signals at 290, 0, and −144.4 ppm (Figure 1) attributable to the perchlorate ion, bulk water, and water coordinated to Rh^{3+} were observed in all samples containing $[Rh(H_2O)_6]^{3+}$. The chemical shift of water in the first coordination sphere of rhodium relative to pure water was obtained from the solution containing only $[Rh(H_2O)_6](ClO_4)_3$. If chromium was added to the solution, all signals were shifted by the same amount relative to the spectrometer frequency due to magnetic susceptibility changes. The chemical shift difference of the bulk water signal in solutions with and without $[Cr(H_2O)_6]^{3+}$ was measured relative to the $[Rh(H_2O)_6]^{3+}$ resonance and reported relative to the pure water shift which was set to zero. All chemical shifts were obtained from fittings of Lorentzian lines to the signals.

NMR Data Treatment and Results

1. Equations. The behavior of NMR relaxation rates and chemical shifts in the presence of dilute paramagnetic species is well known.[34,35] Equations 1−3 describe the relaxation

$$\frac{1}{T_{1r}} = \frac{1}{P_m}\left[\frac{1}{T_1} - \frac{1}{T_{1A}}\right] = \frac{1}{T_{1m} + \tau_m} \tag{1}$$

$$\frac{1}{T_{2r}} = \frac{1}{P_m}\left[\frac{1}{T_2} - \frac{1}{T_{2A}}\right] = \frac{1}{\tau_m}\left[\frac{{T_{2m}}^{-2} + {\tau_m}^{-1}{T_{2m}}^{-1} + {\Delta\omega_m}^2}{({\tau_m}^{-1} + {T_{2m}}^{-1})^2 + {\Delta\omega_m}^2}\right] \tag{2}$$

$$\Delta\omega_r = \frac{1}{P_m}(\omega_{Cr} - \omega_A) = \frac{1}{P_m}(\Delta\omega) = \frac{\Delta\omega_m}{(1 + \tau_m T_{2m}^{-1})^2 + {\tau_m}^2{\Delta\omega_m}^2} \tag{3}$$

enhancement, $1/T_{1,2r}$, the chemical shift variation, $\Delta\omega_r$, as a function of the concentration of the paramagnetic species (expressed as a mole fraction, P_m), the relaxation and shift in the absence of chemical exchange ($1/T_{1,2A}$ and ω_A for the bulk solvent and $1/T_{1,2m}$ and $\Delta\omega_m$ for the bound solvent), and the lifetime, τ_m, of a solvent molecule in the vicinity of the paramagnetic center. $1/T_1$ and $1/T_2$ are the observed longitudinal and transverse relaxation rates. These equations were primarily developed for exchange of solvent molecules between the first coordination sphere and the bulk of the solvent. If the first coordination sphere is kinetically inert, they can be applied to describe the exchange between the second coordination sphere and the bulk.

In the case of very fast exchange ($1/T_{1,2m} \ll 1/\tau_m$; $\Delta\omega_m \ll 1/\tau_m$) eqs 1−3 reduce to

$$\frac{1}{T_{jr}} = \frac{1}{P_m}\left[\frac{1}{T_j} - \frac{1}{T_{jA}}\right] = \frac{1}{T_{jm}} = \frac{1}{T_{jq}} + \frac{1}{T_{jd}} + \frac{1}{T_{jsc}} \quad j = 1, 2 \tag{4}$$

$$\Delta\omega_r = (1/P_m)\Delta\omega = \Delta\omega_m \tag{5}$$

where $1/T_{jq}$ is the quadrupolar, $1/T_{jd}$ the dipolar, and $1/T_{jsc}$ the scalar contributions to the relaxation rates. The chemical shift of the bound water molecules is determined by the scalar interaction between the Cr^{3+} electron spin and the ^{17}O nucleus, which is given by eq 6,[36] where g_L is the isotropic Landé factor

$$\Delta\omega_m = \frac{g_L\mu_B S(S+1)B}{3k_B T}\left(\frac{A}{\hbar}\right) \tag{6}$$

($g_L = 2$ for Cr^{3+}), μ_B is the Bohr magneton, k_B is the Boltzmann constant, S is the electronic spin ($S = 3/2$ for Cr^{3+}), $A/\hbar$ is the hyperfine or scalar coupling constant, and B is the magnetic field. The contribution due to the dipolar interaction[37] is negligible for Cr^{3+} ions in a symmetric environment.[38]

If we assume that the ^{17}O relaxation rates of bulk water, $1/T_{jA}$, are governed by quadrupolar interaction, the difference between

(29) Vold, R. V.; Waugh, J. S.; Klein, M. P.; Phelps, D. E. *J. Chem. Phys.* **1968**, *48*, 3831.
(30) Meiboom. S.; Gill, D. *Rev. Sci. Instrum.* **1958**, *29*, 688.
(31) Plane, R. A.; Taube, H. *J. Chem. Phys.* **1952**, *56*, 33.
(32) Hunt, J. P.; Taube, H. *J. Chem. Phys.* **1951**, *19*, 602.
(33) Xu, F.-C.; Krouse, H. R.; Swaddle, T. W. *Inorg. Chem.* **1985**, *24*, 267.
(34) Zimmermann R.; Brittin, W. E. *J. Phys. Chem.* **1957**, *61*, 1328.
(35) Swift, T. J.; Connick, R. E. *J. Chem. Phys.* **1962**, *37*, 307.
(36) Solomon, I.; Bloembergen, N. *J. Chem. Phys.* **1956**, *25*, 261. Bloembergen, N. *J. Chem. Phys.* **1957**, *27*, 572.
(37) LaMar, G. N.; Horrocks, W. D., Jr.; Holm, R. N. *NMR of Paramagnetic Molecules*; Academic Press: New York, 1973.
(38) Abragam, A. *The Principles of Nuclear Magnetism*; Oxford University Press: London, 1961.

measured transverse and longitudinal relaxation rates is in the case of very fast exchange given by eq 7. In the limit of extreme

$$\frac{1}{T_2}-\frac{1}{T_1}=\frac{1}{P_m}\left[\frac{1}{T_{2q}}+\frac{1}{T_{2d}}+\frac{1}{T_{2sc}}-\frac{1}{T_{1q}}-\frac{1}{T_{1d}}-\frac{1}{T_{1sc}}\right] \quad (7)$$

narrowing, which is certainly valid in this case, the quadrupolar relaxation is given by eq 8.[38] χ is the quadrupole coupling

$$\frac{1}{T_{1q}}=\frac{1}{T_{2q}}=\frac{3\pi^2}{10}\frac{2I+3}{I^2(2I+1)}\chi^2(1+\eta^2/3)\tau_c \quad (8)$$

constant, η the asymmetry parameter, and τ_c the reorientational correlation time of the complex. The longitudinal and transverse dipolar relaxation rates are given by[36,37]

$$\frac{1}{T_{1d}}=\frac{1}{15}\left(\frac{\mu_0}{4\pi}\right)^2\frac{\hbar^2\gamma_I^2\gamma_s^2}{r^6}S(S+1)\left[6\tau_{d1}+14\frac{\tau_{d2}}{1+\omega_s^2\tau_{d2}^2}\right] \quad (9)$$

$$\frac{1}{T_{2d}}=\frac{1}{15}\left(\frac{\mu_0}{4\pi}\right)^2\frac{\hbar^2\gamma_I^2\gamma_s^2}{r^6}S(S+1)\left[7\tau_{d1}+13\frac{\tau_{d2}}{1+\omega_s^2\tau_{d2}^2}\right] \quad (10)$$

$$\tau_{di}^{-1}=\tau_m^{-1}+T_{ie}^{-1}+\tau_c^{-1} \quad i=1,2$$

where $\omega_s=\gamma_s B$ is the electron spin resonance frequency, $\gamma_s=g_L\mu_B/\hbar$ is the electron gyromagnetic ratio, γ_I is the nuclear gyromagnetic ratio ($\gamma_I=-3.626\times10^7$ rad s^{-1} T^{-1} for ^{17}O), r is the effective distance between the electron spin and the ^{17}O nucleus (the metal−oxygen distance in the point dipole approximation),[39] and $1/T_{1e}$ and $1/T_{2e}$ are the longitudinal and transverse electronic relaxation rates. At low magnetic field (<2 T) and approximately room temperature $1/T_{1e}{}^{-1}$ and $1/T_{2e}{}^{-1}\approx10^9$ s^{-1}.[40−42] At higher magnetic fields, as used in our study for example, $1/T_{1e}$ and $1/T_{2e}$ are even smaller. The rotational correlation time of water molecules in the second coordination sphere of $[Cr(H_2O)_6]^{3+}$ which are bound by hydrogen bonds to other water molecules in the first coordination sphere was assumed to be on the order of magnitude of that of bulk water, $\tau_c\approx(2-3)\times10^{-12}$ s. The lifetime of a second sphere water molecule is limited on the fast side by translational diffusion which can be estimated from $\tau_d=d^2/6D$ as 3×10^{-12} s. A rough calculation shows that the dipolar interaction contributes at most 2% to the total relaxation rates as long as $\tau_c>2\times10^{-11}$ s. According to this calculation, the difference between the dipolar contributions, $1/T_{2d}-1/T_{1d}$, has been neglected in a first approximation. This hypothesis has been verified on the basis of our results.

The scalar contribution to the relaxation rates is given by[36]

$$\frac{1}{T_{1sc}}=\frac{S(S+1)}{3}\left(\frac{A}{\hbar}\right)^2\left[\frac{2\tau_{2s}}{1+(\omega_I-\omega_s)^2\tau_{2s}^2}\right] \quad (11)$$

$$\frac{1}{T_{2sc}}=\frac{S(S+1)}{3}\left(\frac{A}{\hbar}\right)^2\left[\tau_{1s}+\frac{\tau_{2s}}{1+(\omega_I-\omega_s)^2\tau_{2s}^2}\right] \quad (12)$$

where $\tau_{js}^{-1}=\tau_m^{-1}+T_{je}^{-1}$ ($j=1,2$). As already mentioned above, in the case of $[Cr(H_2O)_6]^{3+}$, the electronic relaxation is relatively slow, $\tau_m\geq10^{-11}$ s and the NMR experiments were performed at high magnetic field so that $\omega_s\tau_{2s}\gg1$. Equation 7 can therefore be simplified to

$$\frac{1}{P_m}\left[\frac{1}{T_2}-\frac{1}{T_1}\right]\cong\frac{1}{P_m}\frac{1}{T_{2sc}}=\frac{S(S+1)}{3}\left(\frac{A}{\hbar}\right)^2\tau_{1s} \quad (13)$$

Electron spin relaxation of $[Cr(H_2O)_6]^{3+}$ is governed by the modulation of the quadratic zero field splitting (ZFS) interaction and the transverse relaxation rate, $1/T_{1e}$, can be expressed as[40,43]

$$\frac{1}{T_{1e}}=C\left[\frac{\tau_v}{1+\omega_s^2\tau_v^2}+\frac{4\tau_v}{1+4\omega_s^2\tau_v^2}\right] \quad (14)$$

where C is a constant given for the aqua ion and τ_v is the characteristic correlation time for the relaxation whose temperature dependence is given by Arrhenius law

$$\tau_v=\tau_v^{298}\exp(E_v/R(1/T-1/298)) \quad (15)$$

with E_v being the activation energy.

The inverse of the lifetime of a water molecule in the second coordination sphere is equal to the rate of exchange, k_{ex}, and its temperature dependence is assumed to obey the Eyring equation (16), where $\Delta S^\ddagger$ and $\Delta H^\ddagger$ are, respectively, the entropy and enthalpy of activation for the exchange process and k_{ex}^{298} is the exchange rate constant at 298 K.

$$k_{ex}=\frac{1}{\tau_m}=\frac{k_BT}{h}\exp\left(\frac{\Delta S^\ddagger}{R}-\frac{\Delta H^\ddagger}{RT}\right)=\frac{k_{ex}^{298}}{298.15}\times\exp\left[\frac{\Delta H^\ddagger}{R}\left(\frac{1}{298.15}-\frac{1}{T}\right)\right] \quad (16)$$

2. Data Treatment and Results. The enhancement of the oxygen-17 NMR relaxation due to interaction with the paramagnetic ion is relatively small compared to the relaxation of water in the absence of chemical exchange. In order to minimize experimental errors, the measured ^{17}O NMR relaxation rate difference $1/T_2-1/T_1$ has been taken as the difference $(1/T_{2Cr}-1/T_{2Rh})-(1/T_{1Cr}-1/T_{1Rh})$, where $1/T_{2Cr}$ and $1/T_{1Cr}$ are the relaxation rates measured in the mixed chromium and rhodium solutions and $1/T_{2Rh}$ and $1/T_{1Rh}$ are the relaxation rates measured in the pure rhodium solution under exactly the same experimental conditions. Theoretically, the simple difference $1/T_{2Cr}-1/T_{1Cr}$ should give identical results. The method of double difference allows the correction of slight systematic instrumental errors in the measurement of T_1 or T_2, especially in this case where the measured effects are weak and different spectrometers and probeheads were used.

The reduced chemical shifts $\Delta\omega_r$ and relaxation rate difference $1/P_m(1/T_2-1/T_1)$ are shown in Figure 2. The agreement between the experimental points stemming from samples with different Cr/Rh ratios shows that the presence of rhodium does not noticeably affect the chromium second sphere chemical shift and relaxation rate. Nonlinear least squares fits using eqs 5, 6, and 13−16 were performed. In the first instance the parameters governing the electronic relaxation, C, τ_v, and E_v (eq 14), were fixed at values obtained from the literature,[40] $C=1.3\times10^{-20}$, $\tau_v^{298}=3.27\times10^{-12}$ s, and $E_v=8.8\times10^3$ J/mol. The three fitted parameters were $A/\hbar$, $\Delta H^\ddagger$, and $\Delta S^\ddagger$ or k_{ex}^{298}. The fitted curves are represented in Figure 2, and the results of the fits are reported in Table 2.[44]

(39) Kowalewski, J.; Nordenskiöld, L.; Benetis N.; Westlund, P.-O. *Prog. Nucl. Magn. Reson. Spectrosc.* **1985**, *17*, 141.
(40) Melton, B. F.; Pollack, V. L. *J. Phys. Chem.* **1969**, *73*, 3669.
(41) Rubinstein, M.; Baram A.; Luz, Z. *Mol. Phys.* **1971**, *20*, 67.
(42) Levanon, H.; Charbinsky, S.; Luz, Z. *J. Chem. Phys.* **1970**, *53*, 3056.
(43) Bloembergen, M.; Morgan, L. O. *J. Chem. Phys.* **1961**, *34*, 842.
(44) The fit of the data was also repeated with a dipolar contribution to the relaxation rates consisting in eqs 9 and 10. No noticeable change in the fit of the experimental data and the fitted parameters was observed.

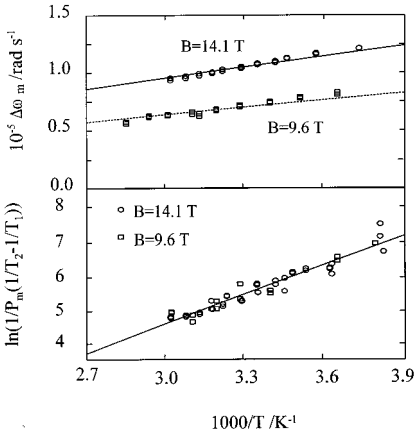

Figure 2. Variable-temperature ^{17}O NMR data for $[Cr(H_2O)_6](ClO_4)_3$/$[Rh(H_2O)_6](ClO_4)_3$ aqueous solutions: reduced chemical shifts and ln$(1/P_m(1/T_2 - 1/T_1))$ at 81.33 MHz (○) and 54.22 MHz (□).

Table 2. Kinetic and NMR Parameters of Water Exchange on the Second Coordination Shell of $[Cr(H_2O)_6]^{3+}$

	$(A/\hbar)$/ (10^6 rad s^{-1})	k_{ex}^{298}/s^{-1}	$\Delta H^{\ddagger}$/ (kJ mol^{-1})	$\Delta S^{\ddagger}$/ (J K^{-1} mol^{-1})
this work	1.349 ± 0.007	$(7.8 \pm 0.2) \times 10^9$	21.3 ± 1.1	$+16.2 \pm 3.7$
Earl[a]	1.5	7×10^9	12	−7

[a] Reference 25; Earl gives in his thesis $A/\hbar = 2.26 \times 10^6$ rad s^{-1}, $k_{ex}^{298} = 10 \times 10^9$ s^{-1}, $\Delta H^{\ddagger} = 2.8$ kcal mol^{-1}, and $\Delta S^{\ddagger} = -0.8$ eu, which were calculated with a second shell coordination number of 8 instead of 12.

The values obtained are in good agreement with the assumption of a very fast exchange ($(T_{2m}\tau_m)^{-1} \gg T_{2m}^{-2}$ and $\Delta\omega_m^2$), and the use of eqs 4, 5, and 7 is well justified. The fit of the data was repeated, allowing the parameters governing the electronic relaxation (C, τ_v^{298}, E_v) to be adjusted by the program. The results of the kinetic parameters and of $A/\hbar$ were unchanged which shows that the correlation time τ_{1s} is dominated by the exchange rate $k_{ex} = 1/\tau_m$ at the high magnetic fields used in our study. The measured scalar coupling constant, $A/\hbar$, was much smaller than first shell values observed for other first row transition metals (Mn^{2+}, 3.3×10^7 rad s^{-1}; Ni^{2+}, 12.3×10^7 rad s^{-1}).[45−47] One can calculate (eqs 14−16) that at low temperature, around 273 K, $1/T_{1e}$ contributes less than 1% to τ_{1s} at 14.1 and 9.4 T, but the contribution increases to about 20% at 1.4 T. Thus, τ_{1s} is reduced to τ_m in eqs 13 and 14 and can be eliminated in the fitting procedure. However, this is not the case at low field (1.4 T) as was used by Earl in a preliminary study.

At room temperature, the different contributions to the observed transverse relaxation rate, $1/T_2$, have been evaluated. The quadrupolar mechanism contributes about 76% to the total relaxation, the scalar mechanism about 21%, and the dipolar mechanism about 3%. The dipolar contribution is on the order of magnitude of the experimental error, and the kinetic information is obtained entirely from the scalar relaxation part.

Density Functional Calculations on $[Cr(H_2O)_6]^{3+}$

Computational Method. To be able to perform molecular dynamics (MD) simulations on the second coordination sphere of the chromium(III) ion, we needed detailed information on the first coordination sphere. We therefore performed calculations within the linear combination of Gaussian type orbitals−density functional (LCGTO-DF) formalism[48−50] using the deMon program package.[51,52] The equilibrium geometries have been obtained by applying the analytical expression for the LCGTO-DF energy gradients.[53] Preliminary geometry optimizations employed the Vosko−Wilk−Nusair (VWN) local spin density exchange-correlation potential.[54] In a second stage, nonlocal gradient correction terms as suggested by Becke for exchange[55] and by Perdew for correlation[56] functionals (BP) have been used, and the geometries were recomputed. Indeed, these corrected functionals have been shown previously to improve relative energies and properties considerably over the local density approximation (LDA).

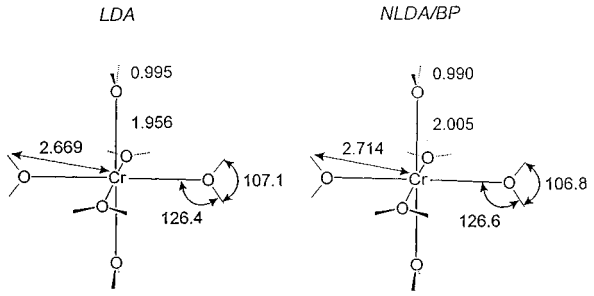

Figure 3. Optimized geometries of $Cr(H_2O)_6^{3+}$, assuming T_h symmetry, for both LDA (left) and NLDA/BP (right) cases. Distances in angstroms, bond angles in degrees.

The "all electron" Gaussian orbital basis set that was used is a 15s/9p/5d set contracted to (63321/5211/41) for chromium, a 9s/6p/1d set contracted to (5211/411/1) for oxygen, and a 5s/1p set contracted to (41/1) for hydrogen.[57] The electron density and exchange-correlation potential were fitted using the following auxiliary bases: Cr(5,5; 5,5), O(5,2; 5,2), H(5,1; 5,1). Our convergence criterion on the total energy for the SCF part of the computations was 10^{-6} hartree. In geometry optimizations, the Broyden−Fletcher−Goldfarb−Shanna algorithm was chosen with a requested accuracy on the norm of the gradient of 10^{-3} au.

Results and Discussion. To reduce the computational effort, the geometry of the $[Cr(H_2O)_6]^{3+}$ complex has been optimized under the constraint of T_h symmetry, and the results are presented in Figure 3 for both LDA and non-LDA (NLDA) cases. As expected, it is seen that the introduction of a nonlocal correction leads to a significant lengthening of the $Cr-O_I$ bond distance (+0.049 Å, O_I and O_{II} are water oxygens in the first and second coordination shells, respectively), the internal geometry of the water molecules being practically the same in both calculations. The increase in the $Cr-O_I$ bond distance on going from LDA to NLDA approximations is a characteristic feature of DF calculations performed for coordination compounds.[58,59] The $Cr-O_I$ bond distances reported in Figure 3

(45) Due to the very slow exchange of first sphere water on $[Cr(H_2O)_6]^{3+}$ no ^{17}O $-A/\hbar$ values are known for Cr^{3+}.
(46) Ducommun, Y.; Newman, K. E.; Merbach, A. E. *Inorg. Chem.* **1980**, *19*, 3696.
(47) Ducommun, Y.; Earl, W. L.; Merbach, A. E. *Inorg. Chem.* **1979**, *18*, 2754.
(48) Sambe H.; Felton, R. H. *J. Chem. Phys.* **1975**, *62*, 1122.
(49) Dunlap, B. I.; Connolly, J. W. D.; Sabin, J. R. *J. Chem. Phys.* **1979**, *71*, 3396.
(50) Andzelm, J.; Radzio E.; Salahub, D. R. *J. Chem. Phys.* **1985**, *83*, 4573.
(51) St-Amant, A.; Salahub, D. R. *Chem. Phys. Lett.* **1990**, *169*, 387.
(52) Salahub, D. R.; Fournier, R.; Mlynarski, P.; Papai, I.; St-Amant, A.; Ushio, J. In *Density Functional Methods in Chemistry*; Labanowski, J. K., Andzelm, J. W., Eds.; Springer: New York, 1991; p 77.
(53) Fournier, R.; Andzelm, J.; Salahub, D. R. *J. Chem. Phys.* **1989**, *90*, 6371.
(54) Vosko, S. H.; Wilk, L.; Nusair, M. *Can. J. Phys.* **1980**, *58*, 1200.
(55) Becke, A. D. *Phys. Rev. A* **1988**, *38*, 3098.
(56) Perdew, J. P. *Phys. Rev. B* **1986**, *33*, 8822; erratum **1986**, *34*, 7406.
(57) Godbout, N.; Salahub, D. R.; Andzelm J.; Wimmer, E. *Can. J. Chem.* **1992**, *70*, 560.
(58) Sosa, C.; Andzelm, J.; Elkin, B. C.; Wimmer, E.; Dobbs K. D.; Dixon, D. A. *J. Phys. Chem.* **1992**, *96*, 6630.

Table 3. Atomic Charges Calculated for the $[Cr(H_2O)_6]^{3+}$ System Using Various Techniques

	q_{Cr}	q_O	q_H
LDA, Mulliken[a]	+1.278	−0.204	+0.246
NLDA, Mulliken[a]	+1.403	−0.167	+0.216
NLDA, MEP[b]	+0.722	−0.627	+0.503

[a] Gross charges derived from a Mulliken population analysis. [b] Charges derived from the molecular electrostatic potential (MEP) according to the procedure suggested by Singh and Kollman (ref 61).

(LDA, 1.956 Å; NLDA, 2.005 Å) may be compared with experimental values as summarized in Table 1. The LDA result is seemingly in better agreement with $Cr-O_I$ distances measured on solids, whereas NLDA results are closer to those observed with different X-ray scattering techniques in aqueous solutions. Our calculations have been performed for gas phase systems, and both crystal packing and lattice effects in crystals may well account for the 0.05 Å discrepancy with NLDA results. It is interesting in this context to report that Åkesson *et al*. have obtained a $Cr-O_I$ bond distance of 2.025 Å for the same complex using the *ab initio* SCF procedure,[60] and their calculations are therefore in good agreement with our NLDA result.

Finally, Table 3[61] presents the atomic charges calculated for the $[Cr(H_2O)_6]^{3+}$ system using various techniques. It was indispensable to derive these charges so as to perform the molecular dynamics calculations reported below. It is seen in Table 3 that the Mulliken population analysis leads to a large positive charge on the metal, and to water molecules bearing a rather small charge (LDA, +0.288; NLDA, +0.265). The fact that the metal charge increases in the NLDA calculations, as compared with the LDA case, is probably due to the larger $Cr-O_I$ distance and, consequently, to a reduction of covalent interactions. Charges derived from the molecular electrostatic potential method (MEP) developed by Singh and Kollman[61] are strongly different from the Mulliken ones: the charge on metal is reduced by roughly 50%, whereas those on both oxygen and hydrogen atoms increase significantly. This result is in agreement with previous calculations attempting to compare the charges obtained for various compounds using several techniques,[62] and concluding that MEP derived charges may be substantially different from Mulliken ones. If we want to describe the electrostatic interactions between the atoms of $[Cr(H_2O)_6]^{3+}$ and further shells of solvent molecules, the MEP derived charges are more adequate descriptors of the charge distribution of $[Cr(H_2O)_6]^{3+}$ because the method was developed to mimic the electrostatic potential at various surface points of a molecule. As the MEP derived charges on oxygen and hydrogen are significantly larger than Mulliken ones, they should lead to a different arrangement of the water molecules of the second coordination sphere by favoring the formation of stronger hydrogen bonds.

Molecular Dynamics Simulation of an Aqueous Solution of $[Cr(H_2O)_6]^{3+}$

Simulation Outline. NPT molecular dynamics simulations were performed on a Silicon Graphics Power Indigo 2 workstation using the program package AMBER 4.0.[63] All interaction potentials in our simulation were of pair potential type and consisted of a Lennard-Jones part (LJ) and a Coulomb part (eq 17). The model is one $[Cr(H_2O)_6]^{3+}$ complex immersed in a periodic box of 277 water molecules together with three perchlorate anions. The bulk and the second sphere water molecules were described by the rigid TIP3P model from Jorgensen et al.[64,65] We abstained from using a flexible water model, which would demand a considerably shorter integration step, but would not substantially improve long-time properties of liquid water.[66] For the geometry and the electric charges of $[Cr(H_2O)_6]^{3+}$ we used the results of our DFT/NLDA/MEP calculations (Figure 3b, Table 3).[67,68] The oxygen atoms were kept fixed at $r_{Cr-O_I} = 2.005$ Å, forming a regular octahedron. The hydrogen atoms of each water molecule, represented by a positive charge $q_{H_I} = +0.503$, were allowed to rotate freely around the water dipole axis which is aligned with the $Cr-O_I$ bond. Due to the strong interaction of the Cr^{3+} ion with the six directly bound oxygen atoms we could not use the Lennard-Jones parameters (R_{O_I}* and ϵ_{O_I}) of the TIP3P model to describe the interaction between a water molecule of the first and a water molecule of the second coordination shell. We therefore carried out nine MD simulations where we varied R_{O_I}* and ϵ_{O_I} systematically, with LJ parameters of Cr^{3+} and the hydrogens fixed to zero. The conditions of these simulations are given in Table 4. The attractive interaction is mainly due to the electrostatic contribution to the interaction potential, and the potential minimum depends strongly on R_{O_I}* but not on ϵ_{O_I}.[69] Table 5 summarizes the most important parameters of nine 100 ps simulations, which were all preceded by equilibration periods

$$E(r) = 4\epsilon\left[\left(\frac{\sigma}{r}\right) - \left(\frac{\sigma}{r}\right)^6\right] + \frac{z_i z_j e^2}{4\pi\epsilon_0 r} \quad \sigma = \frac{2R^*}{2^{1/6}} \qquad (17)$$

Table 4. Overview of MD Simulation Parameters for $[Cr(H_2O)_6]^{3+}$ [a]

number of $[Cr(H_2O)_6]^{3+}$ complexes	1
number of ClO_4^- counter ions	3
number of TIP3P molecules	277
concentration/M	0.196
time step Δt/fs	1
simulation time/ps	100
number of stored configurations	2000
cutoff radius/Å	8.5
density/(g/cm^3)	1.05
temperature/K	298
$\epsilon_{O_{anion}}$/(kcal/mol)	1.739 82[b]
$R_{O_{anion}}$*/Å	0.0757[b]
$\epsilon_{Cl_{anion}}$/(kcal/mol)	2.727 58[b]
$R_{Cl_{anion}}$*/Å	0.0402[b]
q_{Cr}	+0.722
q_{O_I}	-0.627
q_{H_I}	+0.503

[a] Relaxation times for temperature and pressure: τ_T/ps = 0.02; τ_p/ps = 0.5 (ref 69). [b] Parameters for the perchlorate ion from ref 71.

(59) Furet E.; Weber, J. *Theor. Chim. Acta* **1995**, *91*, 157.
(60) Åkesson, R.; Petersson, L. G. M.; Sandström M.; Wahlgren, U. *J. Am. Chem. Soc.* **1994**, *116*, 8691.
(61) Singh U. C.; Kollman, P. A. *J. Comput. Chem.* **1984**, *5*, 129.
(62) Wiberg K. B.; Rablen, P. R. *J. Comput. Chem.* **1993**, *14*, 1504.
(63) Pearlman, D. A.; Case, D. A.; Caldwell, J. C.; Seibel, G. L.; Singh, U. C.; Weiner, P. W.; Kollman, P. A. *Amber 4.0*; University of California: San Francisco, 1991.
(64) Jorgensen, W. L.; Chandrasekhar, J.; Madura, J. D.; Impey, R. W.; Klein, M. L. *J. Phys. Chem*. **1983**, *79*, 926.
(65) Kowall, Th.; Foglia, F.; Helm, L.; Merbach, A. E. *J. Am. Chem. Soc.* **1995**, *117*, .
(66) Guàrdia, E.; Padró, J. A., *J. Phys. Chem*. **1990**, *94*, 6049.
(67) From neutron diffraction data (ref 12) a tilt angle of the first shell water molecules of 34° was calculated. In recent papers the meaning of the tilt angle was questioned (ref 68). From X-ray diffraction data a trigonal orientation of first shell water was concluded (ref 12). Charges calculated for the $[Cr(H_2O)_6H_2O]^{3+}$ cluster show that the charges on first shell oxygen and hydrogen increase by at most 7% due to binding of a second shell water molecule.
(68) Enderby, J. E. *Chem. Soc. Rev*. **1995**, *24*, 159.
(69) τ_T and τ_p are the relaxation times effective in the algorithm of Berendsen *et al.* (ref 70) to keep the system at ambient temperature and pressure. The geometries of the water molecules, ClO_4^- (ref 71), and $[Cr(H_2O)_6]^{3+}$ were fixed by the procedure SHAKE (ref 72).

Table 5. MD Simulation Results for Nine 100 ps Simulations of $[Cr(H_2O)_6]^{3+}$ in a Periodic Box with 277 TIP3P Water Molecules: Dependence on the Lennard-Jones Parameters R_{O_I}* and ϵ_{O_I} for Oxygen Atoms in $[Cr(H_2O)_6]^{3+}$

ϵ_{O_I}/ (kcal/mol)		R_{O_I}*/ Å = 1.462	R_{O_I}*/ Å = 1.564	R_{O_I}*/ Å = 1.666
0.232	$r_{Cr-O_{II}}$[a]/Å	3.90	4.01	4.11
	$FWHH_{O_{II}}$[b]/Å	0.27	0.28	0.35
	$r_{O_I-O_{II}}$[c]/Å	2.32	2.42	2.53
	$r_{Cr-H_{II}}$[d]/Å	4.59	4.71	4.74
	CN[e]	12.39	12.96	13.44
	$g(r)_{min}$[f]/Å	4.32	4.46	4.49
	τ_{res}[g]/ps	2.1×10^5	73	16
	D[h]/(m^2 s^{-1})	5.66×10^{-10}	7.82×10^{-10}	1.94×10^{-9}
0.192	$r_{Cr-O_{II}}$/Å	3.89	3.99	4.09
	$FWHH_{O_{II}}$/Å	0.23	0.27	0.31
	$r_{O_I-O_{II}}$/Å	2.30	2.41	2.49
	$r_{Cr-H_{II}}$/Å	4.55	4.70	4.77
	CN	12.32	12.95	13.29
	$g(r)_{min}$/Å	4.3	4.45	4.47
	τ_{res}/ps	2.7×10^5	150	37
	D/(m^2 s^{-1})	7.73×10^{-11}	1.07×10^{-9}	4.68×10^{-10}
0.152	$r_{Cr-O_{II}}$/Å	3.87	3.97	4.03
	$FWHH_{O_{II}}$/Å	0.23	0.25	0.30
	$r_{O_I-O_{II}}$/Å	2.27	2.37	2.47
	$r_{Cr-H_{II}}$/Å	4.58	4.63	4.72
	CN	12.24	12.67	12.86
	$g(r)_{min}$/Å	4.26	4.39	4.43
	τ_{res}/ps	4.5×10^5	183	38
	D/(m^2 s^{-1})	4.11×10^{-10}	1.49×10^{-9}	8.85×10^{-11}

[a] Distance between the chromium ion and the oxygen atoms O_{II}. [b] FWHH is the full width at half height of the peak of the radial distribution function corresponding to the second hydration shell. [c] Distance between the oxygens of the first and the second shells. [d] Distance between the chromium ion and the hydrogen atoms H_{II}. [e] Second shell coordination number. [f] Distance corresponding to the minimum of the radial distribution function between the second and the third hydration shells. [g] Residence time of a particular water molecule in the second shell. [h] Self-diffusion coefficient.

Table 6. Structural and Dynamic Results from a 300 ps MD Simulation of $[Cr(H_2O)_6]^{3+}$ in a Periodic Box with 277 TIP3P Water Molecules and 3 ClO_4^- Anions (ϵ_{O_I}/(kcal/mol) = 0.192, R_{O_I}*/ Å = 1.564)

$r_{Cr-O_{II}}$/Å	3.99	$g(r)_{min}$/Å	4.45
$FWHH_{O_{II}}$/Å	0.27	τ_{res}/ps	144
$r_{O_I-O_{II}}$/Å	2.41	D/(m^2 s^{-1})	5.59×10^{-10}
$r_{Cr-H_{II}}$/Å	4.66	T/K	298.74
CN	12.94	d	1.05

of at least 20 ps.[70−72] Experimental distances for second sphere water molecules are best reproduced with R_{O_I}* = 1.564 Å and ϵ_{O_I} = 0.192 kcal/mol (see Table 1). In order to obtain good statistics, we prolongated the simulation with these parameters for up to 300 ps. All the following results are based on this simulation (Table 6).

Our intermolecular potential between a seventh (second shell) water molecule and the $[Cr(H_2O)_6]^{3+}$ cluster looks similar to the one developed by Pappalardo *et al.*[19] for Monte Carlo simulations of Cr^{3+} ions in water. In both cases, the polarization of the first shell of water molecules is taken into account in the potential of $[Cr(H_2O)_6]^{3+}$ and the second shell waters are not polarized.[73] Our potential has its energy minimum of −33.7 kcal mol^{-1} at an O_I-O_{II} distance of 2.40 Å compared to −37.52 kcal mol^{-1} at 2.53 Å of Pappalardos.[74] A main difference arises from the way the $[Cr(H_2O)_6]^{3+}-H_2O$ interaction potential has been implemented into the simulation programs. Whereas Pappalardo *et al.* in their Monte Carlo simulation kept the first shell of water molecules rigid, we allowed for a rotation of the hydrogens around the water dipole axis.

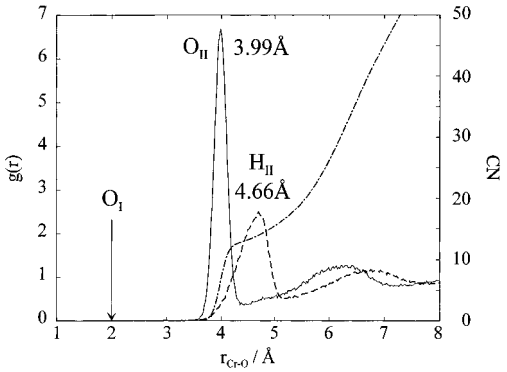

Figure 4. Radial pair distribution function, $g(r)$, and running coordination number, CN, for the simulation with R_O* = 1.564 and ϵ_O = 0.192: $g_{ion-oxygen}(r)$ (—), $g_{ion-hydrogen}(r)$ (- - -), CN(r) (-•-).

Structural Results. The calculated chromium−oxygen and chromium−hydrogen radial distribution functions, $g(r)$, are shown in Figure 4. The position of the first shell oxygens is indicated by an arrow. The peaks at 3.99 Å for the oxygen and at 4.66 Å for the hydrogen corresponding to the second coordination sphere are well-defined. The broad peak at r = 6 Å (6.7 Å for H) corresponds to the third ill-defined coordination sphere. The mean Cr−Cl distance from our simulation is about 7.5 Å, signifying that the perchlorate anions are not sitting in the second coordination sphere but are in the third and beyond. Integration of the oxygen $g(r)$ between 3.00 Å and the first minimum at 4.45 Å gives the mean number of water molecules in the second coordination sphere of Cr^{3+} as 12.94.[75]

The angular orientation of water molecules is shown in Figure 5. Figure 5a illustrates the distribution of the angle θ formed between the water dipole vector and the ion−oxygen distance vector. The strong radial alignment ($\cos(\theta)$ = 1) decreases rapidly from the second coordination sphere to the third and the bulk. Figure 5b shows the distribution angle ω ($\angle O_I-H_I\cdots O_{II}$) of a hydrogen bond between the first and the second hydration shells and reveals a sharp maximum at 180°. Together with the fact that the number of water molecules in the second hydration shell is approximately twice as large as that in the first shell and the dipole moment of water molecules in the second sphere shell is radially aligned (Figure 5a), a picture emerges where each water molecule of the first sphere binds two water molecules by a linear hydrogen bond.

Water Exchange. To obtain the mean lifetime of a water molecule in the second coordination sphere, τ_{res}, we calculated the residence probability, $p(t)$, of a water molecule at a distance of $r_{Cr-O_{II}} \leq 4.45$ Å.[76] The choice of this distance is not straightforward. We have chosen the minimum of $g(r)$ after the peak attributed to the second shell oxygens (Figure 4). The

(70) Berendsen, H. J. C.; Postma, J. P. M.; van Gunsteren, W. F.; DiNola, A.; Haak, J. R. *J. Chem. Phys.* **1984**, *81*, 3684.

(71) Heinje, G.; Luck, W. A. P.; Heinzinger, K. *J. Phys. Chem.* **1987**, *91*, 331.

(72) Ryckaert, J. P.; Ciccotti, G.; Beredsen, H. J. C. *J. Comput. Phys.* **1977**, *23*, 327.

(73) We considered the polarization of the second shell water molecules due to strong hydrogen bonding to first shell water molecules to be negligible. A rough estimation of this effect using DFT calculations showed that the polarization increase compared to water molecules in a dimer is less than 10%.

(74) The complexation energy of the $[Cr(H_2O)_6H_2O]^{3+}$ cluster as obtained from DFT-NLDA calculations is −31.4 kcal mol^{-1} for a geometry corresponding to the minimum of our intermolecular potential function. The same calculation performed on an energy minimized structure (using the DFT-LDA method) ($d_{O_I-O_{II}}$ = 2.438 Å) gave −38.7 kcal mol^{-1}.

(75) The probabilities of finding a coordination number, CN_{II}, of 12 is 0.351, of 13 is 0.418, of 15 is 0.048, and of 16 is 0.004. A CN_{II} smaller than 12 is never observed.

(76) Meier, W.; Bopp, Ph.; Probst, M. M.; Spohr, E.; Lin, J. L. *J. Phys. Chem.* **1990**, *94*, 4672.

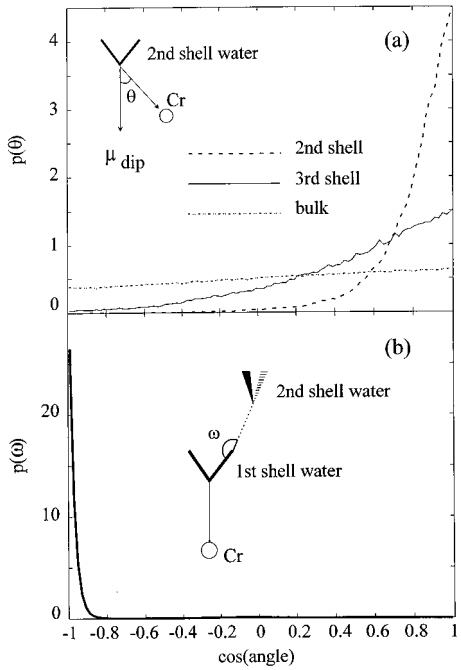

Figure 5. (a) Distribution $p(\theta)$ of the angle θ between the dipole vector of a second sphere water molecule and the ion−oxygen distance vector. (b) Distribution for the angle $\angle O_I-H\cdots O_{II}$ of hydrogen bonds between the first and second solvation shells. For each water molecule in the second sphere (3.00 Å < $r_{ion-oxygen}$ < 4.45 Å) the closest hydrogen atom of a water molecule in the first sphere has been assigned.

residence time τ_{res} obtained by fitting an exponential to $p(t)$ is 144 ps. This time corresponds to the 27 exchanges observed in 300 ps if we account for about 12.94 water molecules in the second sphere. From τ_{res} we calculated an exchange rate for one particular water molecule between the second and the third coordinations shell of $1/\tau_{res} = k_{ex} = 6.9 \times 10^9$ s^1. The $[Cr(H_2O)_6]^{3+}$ diffusion coefficient, D, from our MD simulations (Table 6) agrees well with the experimental value of Easteal *et al.*[21] of $D^{298} = 5.3 \times 10^{-10}$ m^2 s^{-1} extrapolated to low concentrations.

To further analyze the exchange process, we resolved the events into pairs of mutually exchanging water molecules. We have identified from the simulation all transitions between the second solvation shell and the bulk and grouped them into pairs of water molecules that together form a coupled exchange. This was unequivocally possible for 20 out of 27 exchange events. Subsequently, the exchange pathways of these pairs, i.e., the ion−oxygen distance as a function of time, have been smoothed[77] in order to suppress stochastic detail and have then been superposed with respect to a common origin time (Figure 6). The origin is the average between the two times when the leaving and the entering water molecules cross the limit (r = 4.45 Å) between the second and the third solvation spheres. Figure 6 shows that the crossing point of the trajectories of the incoming and of the leaving water oxygens lies close to the mean distance of the second sphere water oxygens. An associative interchange activation mode can therefore be attributed for this exchange reaction.

Further interesting information is obtained from the angular distribution for the angle formed by the two exchanging water molecules (Figure 7). A maximum is found at $\cos(\theta) \approx 0.76$ which means an angle of about 40°. The ion−oxygen distance vectors of two adjacent water molecules in the second coordination sphere produce an angle of about 37° if we take 2.8 Å as a mean distance between the O_{II} oxygens.

(77) Press, W. H.; Flannery, B. P.; Teulolsky, S. A.; Vetterling, W. T. *Numerical recipes*; Cambridge University Press: Cambridge, 1988. NPTS = 4.

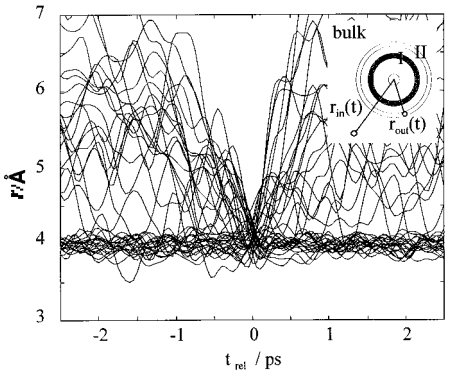

Figure 6. Superposition of the trajectories for 20 exchanges observed between the second shell (II) and the bulk.

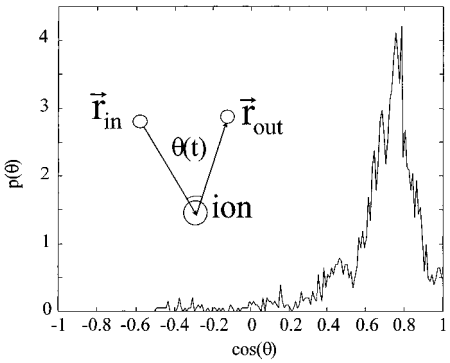

Figure 7. Angular distribution for the angle formed by the entering water molecule, the Cr^{3+} ion, and the leaving water molecule around the moment of an exchange event (−2.5 ps < t < +2.5 ps).

Discussion

Experimental results from earlier diffraction measurements and from our ^{17}O NMR study confirm the presence of a structurally and kinetically well-defined second coordination shell for $[Cr(H_2O)_6]^{3+}$ in aqueous solution. Our molecular dynamics simulations are in good agreement with these experimental observations as well as with a recent Monte Carlo simulation[19] and can therefore be used to obtain more insight into the microscopical picture of the second coordination shell around strongly coordinated cations. The structural picture which results from the computer simulation is as follows. The second coordination shell is composed of 12−15 water molecules in an ion−oxygen distance range of 3.0−4.45 Å.[75] The chromium−oxygen radial distribution function $g_{Cr-O_{II}}$ shows a sharp peak at 3.99 Å (Figure 4) which is equivalent to the mean distance between the ion and the second sphere water oxygens. The mean coordination number obtained from integration over $g(r)$, CN_{II}, is 12.94. The water dipoles in the second shell point radially toward the ionic center (Figure 5a), and the oxygen atoms, O_{II}, form linear hydrogen bonds with hydrogen atoms of first sphere water molecules (H_I, Figure 5b). The O_I-O_{II} mean distance from our simulations is 2.41 Å which compares rather well to 2.6 Å from IR difference spectroscopy[20] and to 2.63 ± 0.09 Å as obtained by means of a geometrical model from large-angle X-ray scattering.[8] The mean distance between a first sphere water proton, H_I, and a second sphere water oxygen, O_{II}, is 1.42 Å (Figure 8) which is considerably shorter than the mean hydrogen bond distance found in neat water (1.8−

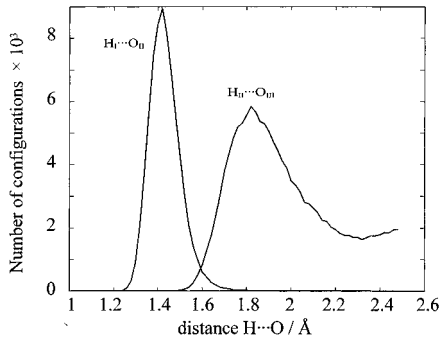

Figure 8. Mean hydrogen−oxygen distances between first and second and second and third coordination shells.

1.9 Å).[78,79] Hydrogen bonds of this length are only possible for extremely strongly bonded systems. Our simulation results are in qualitative agreement with X-ray scattering data from Caminiti *et al.*[9,80] who obtained a better fit by assuming first shell water molecules lying in plane with the Cr^{3+} ion and forming linear hydrogen bonds with second shell water molecules. Furthermore, we agree with Brown[81] who concluded from observations on crystalline hydrates that H bonds connecting H_2O_I and H_2O_{II} molecules are very short and linear. The third shell of water molecules results in a broad peak in the chromium−oxygen radial distribution function at about 6.2 Å. It is composed not only of water molecules but also of oxygens from the three perchlorate anions. The mean Cr−Cl distance from our simulation is 7.5 Å, and during the simulation period of 300 ps ClO_4^- never enters the second coordination shell. The hydrogen bond length between the second and the third coordination shell, $H_{II}-O_{III}$, has its maximum at 1.82 Å (Figure 8) and is therefore within the range found in pure water. From the results of our MD simulation, which are in agreement with experimental radial distribution functions and coordination numbers, we can therefore improve the earlier model proposed by Taube[24] and Earl[25] who assumed that second sphere water molecules are located on the triangular faces of the octahedron formed by the six first sphere H_2O molecules, leading to a coordination number $CN_{II} = 8$.

An interesting result from the MD simulations is the consequence for the first sphere water molecules due to the hydrogen bonding between first and second sphere water. Our theoretical calculations of $[Cr(H_2O)_6]^{3+}$ in the gas phase resulted in T_h symmetry of the water molecules around the ion (Figure 3). The same result is obtained by minimizing the energy of a general 3+ charged ion surrounded by six TIP3P water molecules in the gas phase. The simulations in aqueous solution however led to a different picture for the orientation of the H_I-H_I vector. Figure 9 shows a view of the fist coordination shell of a chromium(III) ion looking along one of the C_4 symmetry axes. The angle ω denotes the angle by which a water molecule is rotated about the O_I-Cr-O_I axes compared to T_h symmetry. The second angle φ defined in Figure 9 is formed by the relative rotation of two first shell water molecules sitting opposite one another within the octahedron. From Figure 10 we find a small preference of angle ω to be ∼45° and for angle φ to be ∼90°. Perhaps we should remind the reader at this point that we set the potential to zero for the rotation of the first sphere water molecules around their dipole axes. The twist of the H_I-H_I vector is therefore a consequence of electrostatic interactions between the first and second coordination shells. A fully rigid model of the first coordination sphere[19] (also keeping the hydrogen atoms fixed in space) cannot show this effect, which, as we will see later, has some significance in the mechanism of water exchange between the second and third coordination shells.

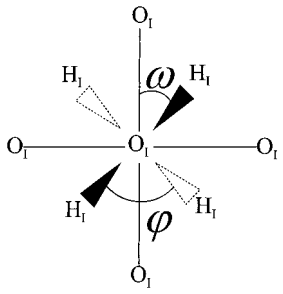

Figure 9. Schematic drawing of the arrangement of water molecules in the first coordination shell of Cr^{3+} (view along a C_4 axis).

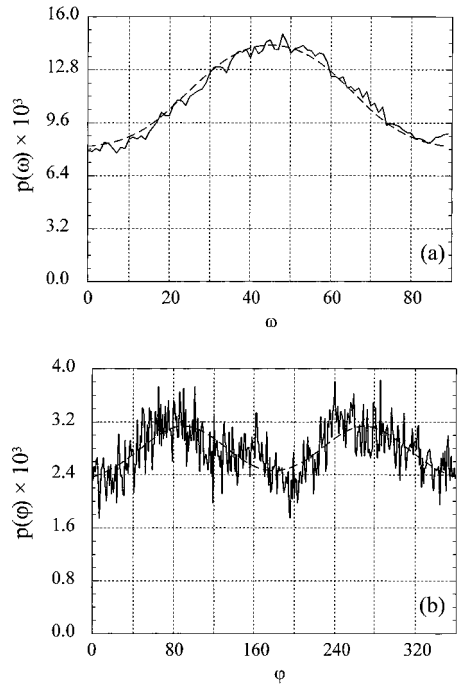

Figure 10. (a) Probability distribution $p(\omega)$ of H_I-H_I vectors of the first shell water molecules as a function of the deviation from T_h symmetry (T_h symmetry corresponds to $\omega = 0°$ or 180°). (b) Probability distribution $p(\varphi)$ of H_I-H_I vectors of opposite first shell water molecules as a function of φ ($\varphi = 0°$ or 180° corresponds to a parallel arrangement of these vectors).

The kinetic parameters for the exchange of water molecules from the second coordination shell obtained by our NMR study are given in Table 2. Whereas the exchange rate constant at 298 K is close to the estimation of Earl (if we recalculate his values with a second shell coordination number of 12), the activation parameters $\Delta H^{\ddagger}$ and $\Delta S^{\ddagger}$ differ substantially; Earl obtained a negative entropy of activation while we measured a positive one. The exchange rate itself is only 1 order of magnitude greater than the fastest exchange rate measured for water exchange from the first coordination sphere of a triply charged cation ($k_{ex}^{298} = 8.3 \times 10^8\ s^{-1}$ for $[Gd(H_2O)_8]^{3+}$).[3] On the other side, the observed lifetime of 128 ps is considerably longer than typical times calculated from translational diffusion.

(78) Beveridge, D. L.; Mezei, M.; Mehrotra, P. K.; Marchese, F. T.; Ravi-Shanker, G.; Vasu, T.; Swaminathan, S. *Adv. Chem. Ser.* **1983**, *204*, 297.

(79) Mountain, R. D. *J. Chem. Phys.* **1989**, *90*, 1866.

(80) Magini, M.; Licheri, G.; Paschina, G.; Piccaluga, G.; Pinna, G. *X-Ray Diffraction of Ions in Aqueous Solutions: Hydration and Complex Formation*; CRC Press: Boca Raton, FL, 1988; pp 90−91.

(81) Brown, D. I. *Acta Crystallogr.* **1976**, *A32*, 24.

Using eq 18, where $\langle \Delta r^2(t) \rangle$ is the mean-square displacement

$$\langle \Delta r^2(t) \rangle = 6Dt \tag{18}$$

at delay time t and D the self-diffusion coefficient of water (2.3×10^{-9} m^2 s^{-1}), we calculated a time t of $\sim 3 \times 10^{-12}$ s for a water molecule to travel the mean distance between the second and the third coordination shells ($\sim$2 Å). The NMR lifetime is also in agreement with the upper limit obtained by incoherent quasi-elastic neutron scattering ($\tau < 5 \times 10^{-9}$ s).[22]

The lifetime of a water molecule in the second shell of a chromium ion obtained from our MD simulations is 144 ps and confirms the existence of a well-defined second coordination shell. The simulations show the presence of a strong link between the interaction potential $E(r_{O_I-O_{II}})$ and therefore the equilibrium distance between first and second shell oxygens and the obtained exchange rate constant (Table 4). A shortening of 1/10 Å leads to an increase in residence time of 3 orders of magnitude whereas a lengthening of 0.1 Å leads to a 1 order of magnitude decrease in residence time. The mean residence time of 144 ps obtained for a mean distance of $r_{O_I-O_{II}} = 2.41$ Å compares to 12−18 ps obtained for second sphere water molecules around lanthanide(III) ions.[23] This difference between Cr^{3+} and the lanthanide(III) ions was already stressed by Bergström *et al*. These authors concluded that whereas second shell water molecules of Cr^{3+} and Rh^3 form hydrogen bonds of comparable strength compared to those formed by some first sphere water molecules of divalent transition metal cations,[20] no such bonds were observed in the case of lanthanides.[82] The strong hydrogen bonding between the first and second shells in the case of Cr^{3+} is also manifested by the dynamical behavior of the simulated waters in the second sphere. If a geometrical criterion is applied for the definition of a hydrogen bond[83] (O···H distance shorter than 1.9 Å), we find a lifetime of the hydrogen bonds between first and second shell waters of about 100 ps, which is on the order of the lifetime of a water molecule in the second shell. The lifetime of hydrogen bonds between second and third sphere water molecules is much shorter, on the order of 2−3 ps. Tanaka[84] found an average lifetime of >1 ps for hydrogen bonding for "stable water molecules" in a simulation of pure water using a similar interaction potential function (TIPS2). The difference between 12 water molecules in the second shell bound by hydrogen bonding and the coordination number of $CN_{II} = 12.94$ as obtained from integration over $g_{Cr-O_{II}}(r)$ is best explained as follows. First, the value of CN_{II} is dependent on the choice of the upper limit of integration (the outer limit of the second coordination shell) if, as in our case, $g(r) > 0$ at this distance. Second, the picture of 12 hydrogen-bonded water molecules is a static one. Due to dynamic processes bulk water molecules enter for a short period of time the second shell and lead therefore to a slight increase of the mean coordination number.

The satisfactory agreement between structural and dynamic behavior of the simulated environment of $[Cr(H_2O)_6]^{3+}$ in aqueous solution and experimental results leads us to use the simulation trajectories of the water to look at the exchange reaction between a second shell and a third shell water molecule on a microscopic scale. From the simulation the following picture was obtained (Figure 11). In the first step a water molecule (no. 3 in Figure 11) enters the second coordination sphere and increases the coordination number temporarily (Figure 6). In the second step the first sphere water molecule (no. 1), close to the entered one, rotates around its oxygen−chromium bond, one of the hydrogen bonds formed to second sphere waters (no. 4 in Figure 11) breaks up, and a new hydrogen bond to the entered water molecule is formed. During the rotation the second hydrogen bond is maintained. The third step is the leaving of the water molecule which lost its hydrogen bond from the second sphere. This relatively simple picture agrees with the simulation result for the angle of about 40° formed between the exchanging molecules (Figure 7). The activation mode which can be attributed for this reaction from the MD simulation is associative. An attribution of the mechanism from experimental exchange rate data which is normally done via the activation entropy, $\Delta S^{\ddagger}$, obtained from temperature variation of the rate constants (k_{ex}) or, better, from the activation volume, $\Delta V^{\ddagger}$, calculated from the pressure variation of k_{ex} is difficult in our case. The only available temperature variation data (Table 2) lead to a small positive $\Delta S^{\ddagger}$, indicating a more dissociative type of activation, whereas Earl[25] measured a small negative value for $\Delta S^{\ddagger}$ which can be linked to an associative type of activation. But the activation entropies are particularly prone to errors because they are obtained by extrapolation of k_{ex} to infinite temperature and there exists a strong correlation between $\Delta H^{\ddagger}$ and $\Delta S^{\ddagger}$.[7a] Unfortunately no pressure variation data were available until now.

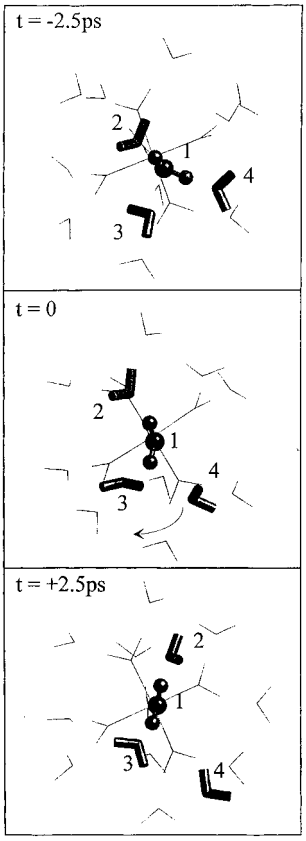

Figure 11. Visualization of a water exchange between the second coordination shell and bulk solvent on $[Cr(H_2O)_6]^{3+}$ obtained from MD simulation.

Conclusion

From our combined experimental and modeling study we find a structurally and kinetically well-defined second coordination shell around chromium(III) ions in aqueous solution. Strong hydrogen bond formation due to polarization of first coordination sphere water molecules leads to a second shell coordination number of 12.94, to short first shell hydrogen−second shell oxygen distances of about 1.4 Å, and to lifetimes of 128 or 144 ps, observed by experiment as well as by simulation. From

(82) Bergström, P.-A.; Lindgren, J. *Inorg. Chem.* **1992**, *31*, 1529.
(83) Mezei, M.; Beveridge, D. L. *J. Chem. Phys.* **1981**, *74*, 622.
(84) Tanaka, H.; Ohmine, I. *J. Chem. Phys.* **1987**, *87*, 6128.

infrared spectroscopy[20] there is also evidence of such strong second shell solvation for other small 3+ ions such as Al^{3+} and Rh^{3+}, whereas for larger 3+ ions like lanthanide(III) or for 2+ ions like Fe^{2+} and Mg^{2+} no such effects were observed.[23,85] The exchange of second shell water molecules takes place between a H_2O molecule which penetrated into the second shell from the bulk of the solution and an adjacent one that leaves after the breaking of its hydrogen bond to the first shell water proton. This exchange procedure is different from what was found by MD simulation of water exchange reactions from very labile first shell water molecules on lanthanide(III) ions.[23] There is no rearrangement of all the molecules belonging to the second shell as was found for the first shell on lanthanide(III) ions. The exchange of second shell and bulk water molecules is a local process and involves only two adjacent molecules. From this point of view the second coordination shell of chromium(III) looks more like a surface where solvent exchange processes are also local events.

(85) Bergström, P.-A.; Lindgren, J. *Inorg. Chem.* **1992**, *31*, 1529.

Acknowledgment. We thank Dr. Thomas Kowall for his technical help and stimulating discussions on the molecular dynamics simulations and Dr. Tomek Wesolowski for performing some supplementary DFT calculations. This work was financially supported by the Swiss National Science Foundation (Grant No. 20-45419.95) and the Swiss OFES as part of the European COST D3 action.

Supporting Information Available: Figure S1, potential energy as a function of the distance between a water molecule of the first solvation sphere and a water molecule of the second sphere, Figure S2, distribution of the number of water molecules in the second coordination sphere, and Figure S3, residence probability $p(t)$ that a water molecule still belongs to the second solvation shell after a correlation time t calculated from MD simulation (4 pages). See any current masthead page for ordering and Internet access instructions.

JA9613116